Tandem gratings spectrometer for spectroscopy broadband anastigmatic imaging

Lei Yu,* Guan-yu Lin, and Shu-rong Wang

Changchun Institute of Optics, Fine Mechanics and Physics, Chinese Academy of Sciences, Changchun 130033, China
**Corresponding author: top1gods@mail.ustc.edu.cn*

Received October 4, 2013; revised December 8, 2013; accepted December 9, 2013;
posted December 13, 2013 (Doc. ID 198942); published January 13, 2014

A tandem gratings spectrometer with high imaging quality is designed. By applying the geometric analysis, the spectral broadband anastigmatic imaging conditions have been obtained. It offers an advanced design with low aberrations for the whole spectral range of the small-scale spectrometer both in the off-axis and coaxial telescope applications. A UV design exhibiting excellent optical performance is presented. The specifications of design have also been investigated. © 2014 Optical Society of America

OCIS codes: (120.4570) Optical design of instruments; (120.6200) Spectrometers and spectroscopic instrumentation; (300.6190) Spectrometers.
http://dx.doi.org/10.1364/OL.39.000351

The imaging spectrometer with reflection gratings supplies multispectral images in one spectral dimension and two spatial dimensions simultaneously, which provides important actions for scientific research and engineering applications. The primary aberration in the imaging spectrometer is the astigmatism. According to the past study, anastigmatic imaging spectrometers can be sorted into several kinds: (1) one-wavelength anastigmatic spectrometers [1,2], as the Czerny–Turner, Ebert–Fastie, and most concave grating spectrometers; (2) two-wavelength anastigmatic spectrometers [3,4], like Offner and Dyson spectrometers; (3) spectrometers of three or more anastigmatic wavelengths [5]. In these designs, special gratings, such as toroidal varied line-space grating and type III holographic concave grating, are used. Whichever imaging spectrometer is adopted, the purpose of the design is to reduce the astigmatism of other wavelengths in the working band to approach the situation of stigmatic wavelength as much as possible.

Conventional tandem gratings imaging spectrometers are generally difficult to satisfy astigmatism-corrected conditions in the spectral broadband. Bartoe and coworkers [6,7] have provided large-scale advanced forms of tandem gratings spectrometers in coaxial telescope applications with excellent performances over a wide spectral range. The two gratings are located to be tangent to a circle of radius of the concave grating. The central light from foreoptics is normally incident on the spectrometer. However, these mountings bring interferences among the optical elements and the detector in the application of small-scale and close spectrometers requesting short focal length. Moreover, the optical imaging quality of these mountings will decrease rapidly in the application of off-axis incidence, such as an off-axis parabolic telescope.

Our research will give a new tandem gratings imaging spectrometer to improve the above inadequacies. In this investigation, the basic tandem mounting is shown in Fig. 1. The off-axis parabolic collimator will adapt to the off-axis and coaxial telescope. The spherical collimator can also be used to save the cost with lower imaging requests. As the incident light onto G_1 is parallel, the following discussion focuses on the tandem gratings.

According to the grating theory given by Beutler [8], the meridian and the sagittal focal distances from G_1 are

$$\begin{cases} r_m = \left[\frac{\cos i+\cos\theta}{R} - \frac{\cos^2 i}{r}\right]^{-1}\cos^2\theta \\ r_s = \left[\frac{\cos i+\cos\theta}{R} - \frac{1}{r}\right]^{-1} \end{cases}. \tag{1}$$

The radius R of $G_1 \to \infty$. As the existence of collimating mirror, the source distance r of $G_1 \to \infty$. So $r_m = r_s = \infty$ for G_1. It decides that the object distance of $G_2 \to \infty$. Therefore, the final meridian and the sagittal focal distances at the imaging plane are

$$\begin{cases} r'_m = R_2\cos^2\theta'(\cos i' + \cos\theta')^{-1} \\ r'_s = R_2(\cos i' + \cos\theta')^{-1} \end{cases}. \tag{2}$$

The distance δ is

$$|\delta| = |r'_m - r'_s| = |R_2\sin^2\theta'(\cos i' + \cos\theta')^{-1}|. \tag{3}$$

When $\theta' = 0$, the astigmatism will be corrected. And the optimum focal distance will be expressed as

$$r' = r'_m = r'_s = R_2(\cos i' + 1)^{-1}. \tag{4}$$

The condition is the optimal Wadsworth condition. In the conventional Wadsworth mounting, it can only be satisfied at one wavelength. But if two tandem gratings are put at the proper positions, the light bundle of each wavelength dispersed in the first order by G_1 which illuminates the relative portion of G_2, will be diffracted in the first order by G_2 along the local normal of the relative section of G_2. At the moment, the condition (4) will be excellently satisfied for all the working wave bands. The tandem mounting presenting spectral broadband anastigmatic images will be investigated.

As shown in Fig. 2, O is the center of curvature and R_2 is the radius of curvature of G_2. $d_{G_1G_2}$ is the distance between the vertex A of G_1 and the local vertex B_1 of G_2. $d'_{G_1G_2}$ is the distance between the vertex A and the local vertex B_2. $d_{G_2I}(B_1I_1)$ is the focal distance from the local vertex B_1 of G_2 to the focal plane I_1I_2. $d'_{G_2I}(B_2I_2)$ is the

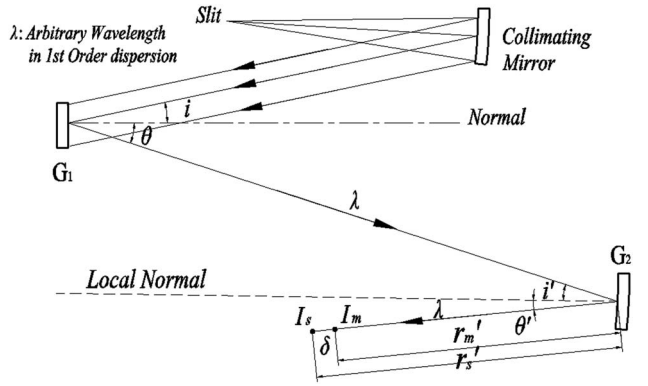

Fig. 1. Tandem gratings mounting. G_1 is the plane grating. G_2 is the concave grating with radius R_2. i and θ are the first incidence and diffraction angles for G_1. i' and θ' are for G_2. I_m and I_s stand for the meridian and sagittal image positions. δ is the distance between them and defines the astigmatic difference. The ruling densities of G_1 and G_2 are identical. r'_m and r'_s are the meridian and sagittal focal distances from G_2.

focal distance from the local vertex B_2 to the focal plane I_1I_2. B_1C_1 and B_2C_2 parallel to the normal of G_1 (SA). AB_1I_1, which is the light path for any wavelength λ, means that λ is dispersed by G_1 in the first order along AB_1 and then is double-dispersed by G_2 in the first order along B_1I_1. AB_2I_2 is similar as AB_1I_1 for λ'. According to the cosine law, the expression will be obtained in the vector triangles AB_1O and AB_2O:

$$d_{G_1G_2}^2 + R_2^2 - 2d_{G_1G_2}R_2 \cos i_1' = d_{G_1G_2}'^2 + R_2 - 2d'_{G_1G_2}R_2 \cos i_2'. \quad (5)$$

It is differentiated with respect to θ_1 and evaluated the resulting expression:

$$(d_{G_1G_2} - R_2 \cos i_1')\frac{dd_{G_1G_2}}{d\theta_1} + d_{G_1G_2}R_2 \sin i_1'\frac{di_1'}{d\theta_1} = 0. \quad (6)$$

When the optimum Wadsworth focal distance

$$d_{G_2I} = R_2(\cos i_1' + 1)^{-1} \quad (7)$$

is satisfied for each wavelength simultaneously, the first-order diffraction angles of all wavelengths from G_2 is equal to zero. Namely, B_1I_1 and B_2I_2 are the local normal lines of G_2. The basic grating equation of G_2 in the first order becomes $g\lambda = \sin i_1'$ (g is the groove density). Then the incidence angle i_1' of G_2 is fixed, which has no relationship with the first-order diffraction angle θ_1 of G_1. Therefore, $di_1'/d\theta_1$ is equal to zero and Eq. (6) becomes

$$(d_{G_1G_2} - R_2 \cos i_1')\frac{dd_{G_1G_2}}{d\theta_1} = 0. \quad (8)$$

With $\overrightarrow{OB_2} - \overrightarrow{OB_1} = \overrightarrow{AB_2} - \overrightarrow{AB_1}$, we have

$$\begin{cases} R_2\cos(\theta_2 - i_2') - R_2\cos(\theta_1 - i_1') = d'_{G_1G_2}\cos\theta_2 - d_{G_1G_2}\cos\theta_1 \\ R_2\sin(\theta_2 - i_2') - R_2\sin(\theta_1 - i_1') = d'_{G_1G_2}\sin\theta_2 - d_{G_1G_2}\sin\theta_1 \end{cases}. \quad (9)$$

By differentiating Eq. (9) with respect to θ_1, we have

$$\frac{dd_{G_1G_2}}{d\theta_1} = d_{G_1G_2}\tan i_1'. \quad (10)$$

Because $i_1' \neq 0$, Eq. (10) is not equal to zero. So the solution of Eq. (8) is

$$d_{G_1G_2} = R_2 \cos i_1'. \quad (11)$$

The expression (11) defines the optimal value of $d_{G_1G_2}$ for the working wave band, which also admits the best focal distance d_{G_2I} is suitable for each wavelength at the same time. These two best distances determine the arrangements of G_1 and G_2. For the sake of convenience for the design, these two distances will be calculated under the first-order dispersed central wavelength.

It should be noticed that the ideal imaging plane is a curved surface for the expression (7) (very close to a plane surface). Hence, the surface of the detector, which is flat, does not strictly accord with the ideal imaging plane. The little marginal defocusing amount will restrict the width of the working wave band within not too broad limits.

As shown in Fig. 3, a proper inclined angle α will make the ideal curved imaging plane S_1S_2 coincide with the actual flat surface I_1I_2 as possible. OI_1 is the half-width of the imaging plane. According to the expression (7) and the basic grating equation $g\lambda = \sin i'$, we have

$$r' = \frac{R_2}{1 + \sqrt{1 - (g\lambda)^2}}. \quad (12)$$

And the inclined angle α is estimated as

$$\alpha \approx \arcsin\left(\frac{r'_{\text{central}} - r'_{\text{min}}}{w/2}\right) = \arcsin\left(\frac{2R_2}{w}\left(\frac{1}{1 + \sqrt{1 - (g\lambda_{\text{central}})^2}} - \frac{1}{1 + \sqrt{1 - (g\lambda_{\text{min}})^2}}\right)\right). \quad (13)$$

The calculation of the optimal angle under the central wavelength makes the estimates much easier but has a little deviation from the ideal value for the curved imaging surface. If the best imaging quality cannot be obtained

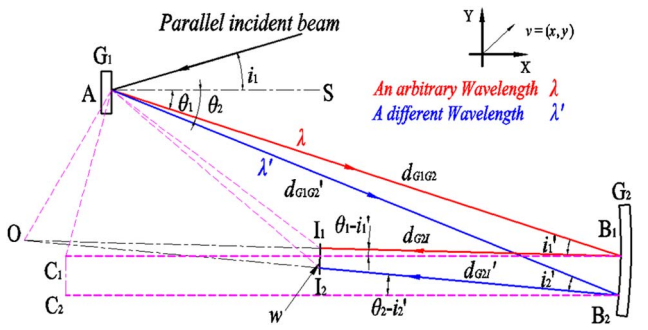

Fig. 2. New advanced tandem gratings spectrometer mounting.

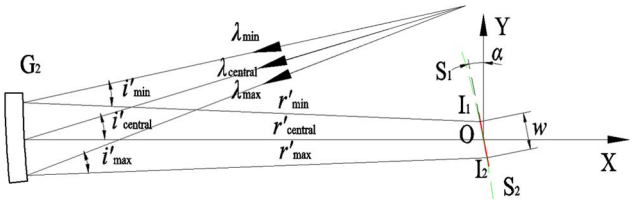

Fig. 3. Sketch of imaging plane. The width of working wave band is $\lambda_{max} - \lambda_{min} \cdot r'$ with different subscript stands for different focal distance. The direction of the distance $r'_{central}$ is also the X direction. The line I_1I_2 stands for the detector plane and the dashed curve S_1S_2 stands for the ideal imaging plane. w is the width of I_1I_2 (usually the width of the detector).

in the actual design, we can adjust the calculated angle a little larger.

Usually, the radius of the concave grating will be fixed according to the focal length of design requests.

According to Fig. 2, the spectral resolution is

$$d\lambda = \frac{d\theta_1}{dw} \cdot \frac{d\lambda}{d\theta_1} \cdot dw \tag{14}$$

$d\theta_1/d\lambda = mg/\cos\theta_1$ is the angular dispersion, where m is the given diffraction order ($m = 1$) and w is the width of imaging plane between two wavelengths. The corresponding minimal dw is

$$dw = \frac{sf_2 \cos i_1 \cos i'_1}{f_1 \cos\theta_1 \cos\theta'_1} \frac{1}{\cos\alpha}, \tag{15}$$

which is also the minimal spectral bandwidth that the imaging spectrometer can distinguish on the imaging plane (the width of slit imaging). f_1 and f_2 are the focal lengths of the collimating mirror and G_2. s is the width of the slit. α is the inclined angle of the imaging plane.

The following relationships are obtained in the vector triangles AB_1C_1, AB_2C_2, and AI_1I_2:

$$\begin{cases} w \cdot \sin(\theta_1 - i'_1) = d'_{G_2I} \cos(i'_2 - \theta_2) - d_{G_2I} \cos(i'_1 - \theta_1) \\ \qquad + d'_{G_1G_2} \cos\theta_2 - d_{G_1G_2} \cos\theta_1 \\ w \cdot \cos(\theta_1 - i'_1) = d'_{G_2I} \sin(i'_2 - \theta_2) - d_{G_2I} \sin(i'_1 - \theta_1) \\ \qquad - d_{G_1G_2} \sin\theta_1 + d'_{G_1G_2} \sin\theta_2 \end{cases}. \tag{16}$$

It is differentiated with respect to θ_1 and we obtain

$$\frac{dw}{d\theta_1} = \frac{R_2(1 + \cos i'_1 + \cos^2 i'_1)}{(1 + \cos i'_1)}. \tag{17}$$

Therefore, with expressions (14), (15), and (17), the spectral resolution of new design is

$$d\lambda = \frac{(1 + \cos i'_1)\cos i_1 \cos i'_1}{(1 + \cos i'_1 + \cos^2 i'_1)\cos\theta'_1 \cos\alpha} \cdot \frac{f_2}{mgR_2f_1} s. \tag{18}$$

According to the expression (18) and the spectral resolution request, the groove density will distribute in a definite range. The relatively suitable one will be chosen to save the cost.

Optimal parameters of the tandem gratings imaging spectrometer design have been confirmed under the central wavelength as

$$\begin{cases} d_{G_2I} = R_2(\cos i'_1 + 1)^{-1} \\ d_{G_1G_2} = \cos i'_1 R \\ \alpha \approx \arcsin\left(\frac{2R}{w}\left(\frac{1}{1+\sqrt{1-(g\lambda_{central})^2}} - \frac{1}{1+\sqrt{1-(g\lambda_{min})^2}}\right)\right) \end{cases}. \tag{19}$$

An example in 260–380 nm for the ultraviolet atmosphere observation in the off-axis telescope application is simulated by ZEMAX in the previous strategy investigated. The central wavelength is chosen as 320 nm. Specifications and performances are shown in Table 1. As

Table 1. Specifications and Performances for the Advanced Tandem Imaging Spectrometer

Specifications	
Spectral range	260–380 nm over 17 mm
Spatial pixel resolution	<0.25 mrad
Spectral resolution	<0.25 nm
F/# number	6.95
Parameters of Design	
Telescope (off-axis parabolic)	Radius 200 mm Off-axis amount 15 mm
Field of view	4° × 0.029°
Collimating mirror (off-axis parabolic)	Same as telescope
Slit	7 mm × 0.05 mm
Plane grating	Ruling density 700 line/mm Incident angle 13°
Concave grating	Ruling density 700 line/mm Incident angle 12.95° Radius 200 mm
$d_{G_1G_2}$	194.87 mm
d_{G_2I}	101.25 mm
α	3.3°
Performances	
RMS spot radii	<11.39 μm
80% encircled energy	10.66 μm
MTF (Nyquist frequency 20 lp/mm)	>0.65

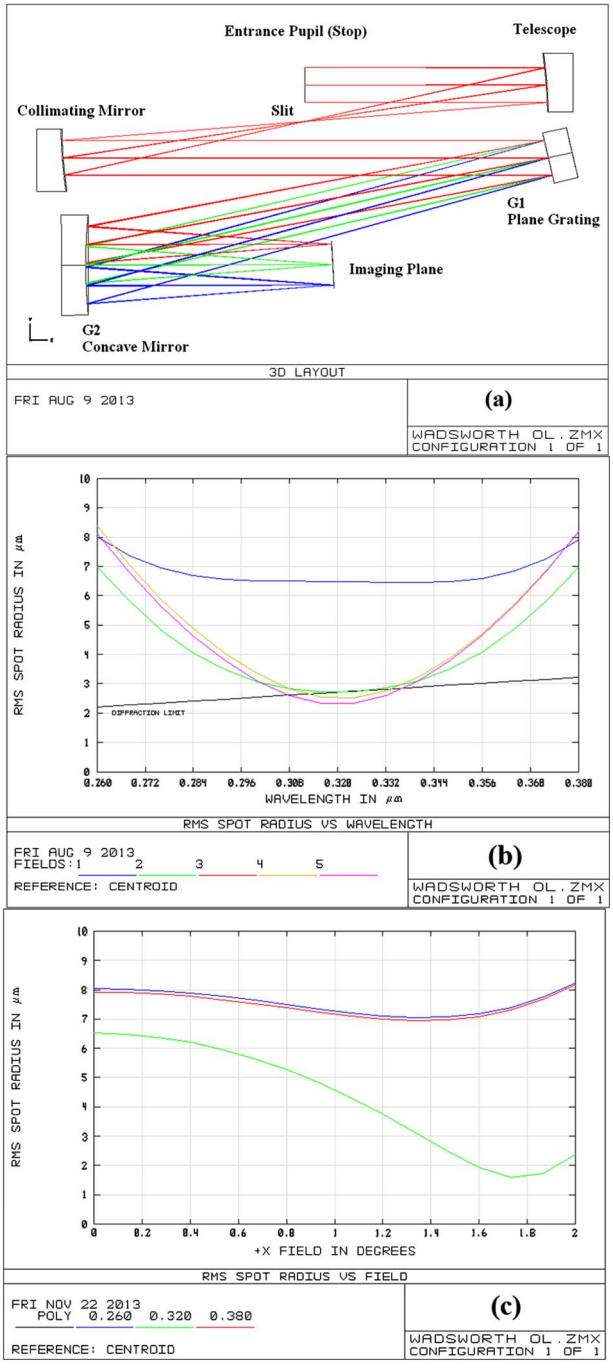

Fig. 4. (a) Sketch of the design. (b) RMS spots radii versus wavelengths in the central and marginal fields of view. (c) RMS spots radii versus fields of view (+X, along the length of slit) in the central and marginal wavelengths.

shown in Fig. 4(b), RMS spots are completely enclosed in a square pixel of side 25 μm and approach the diffraction limit in the working wave band.

In comparison with the other major forms of imaging spectrometers, the new tandem mounting has the following advantageous features for the application:

(1) The new design presents excellent optical performances among similar symmetric systems (the nonconcentric optical system), such as the Czerny–Turner and single-grating (Rowland circle) imaging spectrometer [5,9]. Our design provides the same high spatial resolution but higher spectral resolution under the same parameters as F/# number, field of view, focal length, and ruling density of grating. The mounting is also provided with the best ability of avoiding the stray light.

(2) The concentric system, such as the Offner and Dyson imaging spectrometer, presents better imaging quality under lower F/# number than our design. But there are many restrictions of the configuration [10]. (a) Spectrometers are limited to low dispersion. They are more suitable for the visible-infrared remote sensing with low spectral resolution, such as ocean observation. (b) Transmitting material is required. The existing optical material does not easily satisfy the request of transmission efficiency for the ultraviolet (especially the far and extreme ultraviolet) observation. (c) Gratings are restricted. Gratings in concentric systems are often holographically formed. Its diffracted efficiency is very low for the ultraviolet band. Therefore, the characteristics decide that our designed imaging spectrometer is more suitable for the high precise UV-FUV-EUV spectral observation than the concentric optical system.

To summarize, we present a simple analysis that allows a new tandem gratings imaging spectrometer with broadband high performance in the small-scale and off-axis application. The optimal imaging conditions have been calculated by the geometric method, which determines all the parameters (the arrangement, grating radius, and groove density) of the mounting. It will obtain outstanding stigmatic spectral images in the whole working spectral range. An example for the UV band in 260–380 nm confirms the optical performances of the design. Thus, the new design provides excellent optical quality in a spectral broadband, with a simple and compact device.

References

1. K.-S. Lee, K. P. Thompson, and J. P. Rolland, Opt. Express **18**, 23378 (2010).
2. M. Beasley, C. Boone, N. Cunningham, J. Green, and E. Wilkinson, Appl. Opt. **43**, 4633 (2004).
3. X. Prieto-Blanco, C. Montero-Orille, B. Couce, and R. dela Fuente, Opt. Express **14**, 9156 (2006).
4. C. Montero-Orille, X. Prieto-Blanco, H. Gonzalez-Nunez, and R. dela Fuente, Opt. Lett. **35**, 2379 (2010).
5. L. Yu, S.-r. Wang, Y. Qu, and G.-y. Lin, Appl. Opt. **50**, 4468 (2011).
6. J. D. F. Bartoe and G. E. Brueckner, J. Opt. Soc. Am. **65**, 13 (1975).
7. M. P. Nakada, J. Opt. Soc. Am. **69**, 165 (1979).
8. H. G. Beutler, J. Opt. Soc. Am. **35**, 311 (1945).
9. Q. Xue, S. Wang, and F. Lu, Appl. Opt. **48**, 11 (2009).
10. L. Mertz, Appl. Opt. **16**, 3122 (1977).